Modelling Active Distribution Networks under Uncertainty: Extracting Parameter Sets from Randomized Dynamic Responses

Gilles Chaspierre
Dept. of Elec. Eng. and Comp. Science
University of Liège, Belgium
g.chaspierre@ulg.ac.be

Patrick Panciatici
Research & Development Dept.
RTE, Versailles, France
patrick.panciatici@rte-france.com

Thierry Van Cutsem
Fund for Scientific Research (FNRS)
University of Liège, Belgium
t.vancutsem@ulg.ac.be

***Abstract*—This paper deals with the dynamic modelling of distribution systems hosting a large amount of Inverter-Based Generators (IBGs), more precisely their response to large disturbances in the transmission system. It is assumed that the individual behaviour of IBGs and loads is reasonably well captured by a parameterized model, but the values of its parameters are uncertain. Monte-Carlo simulations involving random variations of those parameters are performed. The dynamic response closest to the average is extracted as being representative. A simple procedure is described to stop the simulations as soon as sufficient information is available. Detailed simulation results are provided, relative to a distribution grid with 75 loads and 75 IBGs. The latter are represented by a generic model that reproduces the main requirements of typical grid codes.**

***Index Terms*—active distribution networks, uncertain dynamic systems, inverter-based generation, Monte-Carlo simulations**

I. Introduction

Distribution networks are expected to host an increasing amount of dispersed generation units exploiting renewable wind or solar energy, and connected through power electronics converters. In many countries, the grid codes are being updated to request those Inverter-Based Generators (IBGs) to provide services, such as supporting the grid voltage and remaining connected in response to normally cleared faults. This will further transform the traditional distribution systems into Active Distribution Networks (ADNs).

Present in large numbers ADNs will modify the dynamics of the combined transmission-distribution system. For instance, it will no longer be justified to replace the distribution systems by passive, equivalent loads when simulating faults in the transmission grid. The first step towards reliable modelling is to set up representative ADN dynamic models. The latter can be used to simulate faults in the distribution grid. To simulate faults occurring in the transmission system, the next step will consist of building equivalents, i.e. reduced-order models of the ADNs. In this paper the focus is on the first step.

One major issue when setting up a detailed ADN model lies in the uncertainty affecting the behaviour of its components. Their dynamic models involve parameters which are not known accurately. This is a well-known fact for loads in general. For instance, it is customary to include an equivalent motor representing the cumulated effects of a population of smaller motors, but its parameters are usually set to "typical" values (e.g. [1]). This is also true for IBGs in so far as the grid codes specify a range of admissible behaviours, leaving the manufacturers with some freedom in the design of their equipments. In this work, it is assumed that the individual dynamic behaviour of IBGs, loads, etc. can be reasonably well captured by a parameterized model, but the values of its parameters are uncertain. Robust control schemes to deal with such uncertainties have been proposed, e.g. in [2], [3].

A well-known approach to deal with such uncertainty consists of performing Monte-Carlo (MC) simulations [4], involving in this case random variations of the parameters. Thus, for given disturbances and operating points, a set of randomized time responses is generated [5]. The next step is to extract from this large set one (or possibly several) representative response(s). The parameters that yielded this response are used in the final ADN model.

This objective bears similarity with the one of [6], where a number of scenarios (obtained by varying load, IBG composition, fault location, etc.) were considered and the ADN active and reactive power responses grouped into a small number of clusters to reduce the computational effort for the derivation of an ADN equivalent. In this paper, uncertainty affects the parameters of the ADN model rather than the scenarios, and a much larger set of randomized responses is considered.

The rest of the paper is organized as follows. The approach for extracting a representative response and choosing the number of MC simulations is given in Section II. The parameterized model used for each load and each IBG, respectively, is presented in Section III, while the simulation results on a test system are given in Section IV. Concluding remarks are offered in Section V.

II. Extracting a representative dynamic response

A. Generating the MC simulations

Consider a distribution network feeding n_L loads and hosting n_G IBGs. For simplicity, and without loss of generality, the same "generic" model is used - though with different parameter values - for each IBG and similarly for the loads.

Let π_G (resp. π_L) be the number of parameters of the IBG (resp. load) model. Thus, the vector $\boldsymbol{p}$ of parameters of the whole ADN model involves $n_G\,\pi_G + n_L\,\pi_L$ components.

Monte-Carlo simulations involve random variations of $\boldsymbol{p}$ with $\boldsymbol{p}^{min} \leq \boldsymbol{p} \leq \boldsymbol{p}^{max}$. The components of $\boldsymbol{p}$ are treated as independent random variables. If no other information is available, it makes sense to make $\boldsymbol{p}$ obey a uniform distribution between the specified bounds $\boldsymbol{p}^{min}$ and $\boldsymbol{p}^{max}$ [5]. Alternatively, the distribution can be centered around the middle of the interval by assuming a truncated Gaussian distribution with average $\boldsymbol{\mu} = (\boldsymbol{p}^{min}+\boldsymbol{p}^{max})/2$ and $(\boldsymbol{p}^{max}-\boldsymbol{p}^{min})/6$ as vector of standard deviations.

Note that the parameters are randomized from one MC simulation to another, but also from one bus to another inside the same MC simulation.

Starting from the same initial operating point, a disturbance is simulated with s instances of the same model corresponding to the randomly drawn parameter vectors $\boldsymbol{p}_1, \ldots, \boldsymbol{p}_s$.

B. Identifying a representative instance of the model

The objective is to extract a simulation representative of the set of s simulations. There is more than one interpretation of the term "representative". It may depend on the type of study, it may not be the same for the distribution system operator as for the transmission one, or it may even be of interest to keep several representative simulations. In this work it has been chosen to : (i) select one dynamic response corresponding to one of the s parameter vectors, (ii) select the one closest to the average of the s responses.

Furthermore, the representative response should not be selected on the basis of a single disturbance, with the risk of over-fitting that particular scenario. Instead, d different disturbances are considered, and a single parameter vector $\boldsymbol{p}^\star$ is going to be extracted for all of them together.

The dynamic simulations involve responses to large disturbances (typically faults) taking place in the transmission system. The variables of interest are the active and reactive powers entering the ADN. Thus, the numerical simulation of the j-th disturbance ($j = 1, \ldots, d$) with parameters $\boldsymbol{p}_i$ yields two time series of n values, respectively $P(\boldsymbol{p}_i, j, k)$ and $Q(\boldsymbol{p}_i, j, k)$, where k refers to the discrete times ($k = 1, \ldots, n$).

Two methods were investigated to identify $\boldsymbol{p}^\star$, the instance of $\boldsymbol{p}$ which fulfills the above requirements.

1) First method: The average power responses are computed as ($j = 1, \ldots, d; k = 1, \ldots, n$):

$$\bar{P}(s, j, k) = \frac{1}{s}\sum_{i=1}^{s} P(\boldsymbol{p}_i, j, k) \quad (1)$$

$$\bar{Q}(s, j, k) = \frac{1}{s}\sum_{i=1}^{s} Q(\boldsymbol{p}_i, j, k) \quad (2)$$

and $\boldsymbol{p}^\star$ is the parameter instance which yields the responses closest to the averages, over all disturbances. It is the solution of the discrete optimization:

$$\min_{\boldsymbol{p}_i \in \{\boldsymbol{p}_1, \ldots, \boldsymbol{p}_s\}} \left\{ \sum_{j=1}^{d}\sum_{k=1}^{n} \left[P(\boldsymbol{p}_i, j, k) - \bar{P}(s, j, k)\right]^2 + \sum_{j=1}^{d}\sum_{k=1}^{n} \left[Q(\boldsymbol{p}_i, j, k) - \bar{Q}(s, j, k)\right]^2 \right\} \quad (3)$$

2) Second method: $\boldsymbol{p}^\star$ is directly identified as the parameter instance which yielded the response to which the other responses have minimal dispersion. This amounts to solving:

$$\min_{\boldsymbol{p}_i \in \{\boldsymbol{p}_1, \ldots, \boldsymbol{p}_s\}} \left\{ \sum_{\substack{\ell=1 \\ \ell \neq i}}^{s}\sum_{j=1}^{d}\sum_{k=1}^{n} \left[P(\boldsymbol{p}_i, j, k) - P(\boldsymbol{p}_\ell, j, k)\right]^2 + \sum_{\substack{\ell=1 \\ \ell \neq i}}^{s}\sum_{j=1}^{d}\sum_{k=1}^{n} \left[Q(\boldsymbol{p}_i, j, k) - Q(\boldsymbol{p}_\ell, j, k)\right]^2 \right\} \quad (4)$$

C. Number of Monte-Carlo simulations

The number of MC simulations must be large enough for the randomly drawn sample to be representative, but not larger owing to the computational burden. It is thus desirable to stop generating randomized responses once sufficient information is contained in the sample.

Keeping in mind that our aim is to extract the average response, the approach consists of increasing the sample until the average power responses, over all disturbances, do no longer vary significantly. The detailed procedure is as follows.

1) Initialize: $s = s_o$, $g = 0$
2) Draw at random an initial set of s_o parameter vectors $(\boldsymbol{p}_1, \ldots, \boldsymbol{p}_{s_o})$
3) for each parameter vector, simulate the ADN response to each of the d disturbances
4) compute the average power responses $\bar{P}(s_o, j, k)$ and $\bar{Q}(s_o, j, k)$
5) generate a new random parameter vector $\boldsymbol{p}_{s+1}$
6) for this parameter vector, simulate the ADN response to the d disturbances
7) compute the new average power responses $\bar{P}(s+1, j, k)$ and $\bar{Q}(s+1, j, k)$
8) compare them with the previous averages by computing the Euclidean distance over all the disturbances:

$$\varepsilon = \sqrt{\varepsilon_P^2 + \varepsilon_Q^2} \quad (5)$$

where:

$$\varepsilon_P^2 = \frac{1}{d\,n}\sum_{j=1}^{d}\sum_{k=1}^{n} \left[\bar{P}(s+1, j, k) - \bar{P}(s, j, k)\right]^2 \quad (6)$$

$$\varepsilon_Q^2 = \frac{1}{d\,n}\sum_{j=1}^{d}\sum_{k=1}^{n} \left[\bar{Q}(s+1, j, k) - \bar{Q}(s, j, k)\right]^2 \quad (7)$$

9) if $\varepsilon \leq \delta$ then $g \to g + 1$; else $g = 0$
10) If $g = g_{max}$ then stop; else $s \to s + 1$. Go to Step 5.

As it can be seen, the procedure starts by performing a set of s_o MC simulations. Simulations are added one by one until ε has remained smaller than the tolerance δ over the last g_{max} simulations.

With this proposed stopping criterion, randomizing more parameters does not necessarily increase the computational burden.

III. Load and IBG generic models

A. Load model

As shown in Fig. 1, each load is split into an equivalent 3rd-order induction motor (taking initially a fraction f of the load active power) and a static part with exponential model.

The randomized parameters are:

- for the motor part: fraction f, three inductances, stator and rotor resistances, inertia constant, fraction of quadratic mechanical torque, initial (capacitor compensated) power factor, and load factor [1]. Different ranges of values are assumed for industrial and residential motors;
- for the static part of the load: exponents α and β.

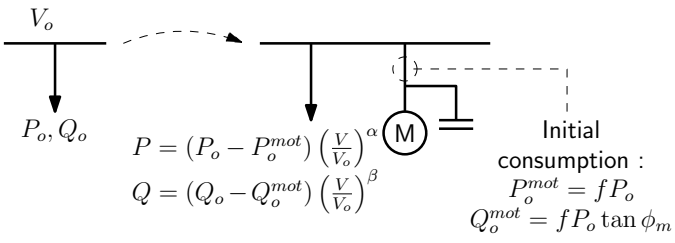

Figure 1. Load composition

B. IBG model

The IBG generic model is given in block-diagram form in Fig. 2. Instead of focusing on internal components, the model aims at reproducing the IBG response to terminal voltage changes required by most grid codes. These requirements and a few other important characteristics are described hereafter. For more details please refer to [7].

1) Low Voltage Ride-Through (LVRT): LVRT capability is an important feature of IBGs, requiring them to remain connected to the grid during a disturbance as long as the voltage is above a reference curve, as shown in Fig. 3. The curve can be adjusted to fit various grid requirements by modifying T_1, T_{int}, T_2, V_{min}, V_{int} and V_r. These parameters were not randomized from one bus to another since it was assumed that the rules in force in the ADN are obeyed by the IBG units.

2) Reactive current injection: In low voltage conditions IBGs are requested to inject reactive current into the grid to support the terminal voltage. The injected current varies linearly with the measured voltage magnitude at the terminal bus, as shown in Fig. 4. Since grid codes usually do not specify one value for the slope k_{RCI} but only a range of values, this parameter has been randomized between 2 and 6, as stated in [8]. On the other hand, m and V_{S1} were not randomized but set to $m = 0$ and $V_{S1} = 0.9$ pu.

3) Active power restoration: When the IBG is called to support the grid voltage as explained in the previous section, it may happen that the active current is reduced to leave room for its reactive counterpart without exceeding the inverter current limit. Once the voltage has recovered to normal values, the IBG gets back to normal operation and, hence, restores its active current. This cannot take place too rapidly but it should not take too much time either, to avoid a power imbalance. This is why some grid codes specify a range of allowed values for the rate of increase of the active current (see e.g. [9]). To account for this dispersion, the rate of change has been randomized between 20 and 50 % of the rated power per second, in accordance with [8].

4) Other randomized parameters: The following parameters, not referred to in grid codes, have been randomized:

- the gain k_{PLL} of the Phase-Locked Loop (PLL) (see Fig. 2), which influences its response time;
- the voltage threshold V_{PLL} below which the PLL is frozen (see Fig. 2);
- the equivalent time constant T_g (see Fig. 2);
- the IBG rated current, to reflect the fact that installed capacities are not known accurately.

The voltage measurement time constant T_m is not varied.

IV. Simulation results

A. Test system and disturbances

The 75-bus 11-kV network considered in [10] has been reused in this study. Its one-line diagram is given in Fig. 5.

Among the 75 MV buses, 38 feed Low-Voltage (LV) distribution grids hosting small residential Photo-Voltaic (PV) units. The corresponding load is 4.7 MW and the production is 1.9 MW. Each MV bus injection is modeled as shown in Fig. 6.a with a lumped load and a lumped PV unit behind an impedance $R_e + jX_e$ accounting for the MV/LV transformer and the LV feeder(s). Both R_e and X_e are randomized. At the remaining 37 MV buses, the injection is modeled by an industrial load and a large PV unit behind a transformer, as shown in Fig. 6.b. These IBGs have fault-ride-through and reactive current injection capabilities, while the ones in the LV grids do not. The parameters of the respective fault-ride-through characteristics are given in Fig. 3. The corresponding load is 24.7 MW and the production is 19.2 MW.

The disturbances considered are severe voltage dips, caused typically by faults, and applied on the transmission side of the main transformer. They are characterized by a duration ΔT and a depth ΔV, as shown in Fig. 7. The values of ΔT and ΔV are given in the same figure for the eight disturbances considered in this paper. $\Delta T = 0.10$ s has been chosen to account for faults cleared by primary protections, and $\Delta T = 0.25$ s for faults cleared by back-up protections.

Simulations were performed with RAMSES, a software for time simulation in phasor mode, developed at the Univ. of Liège [11]. The algorithms presented in Section II were implemented in MATLAB.

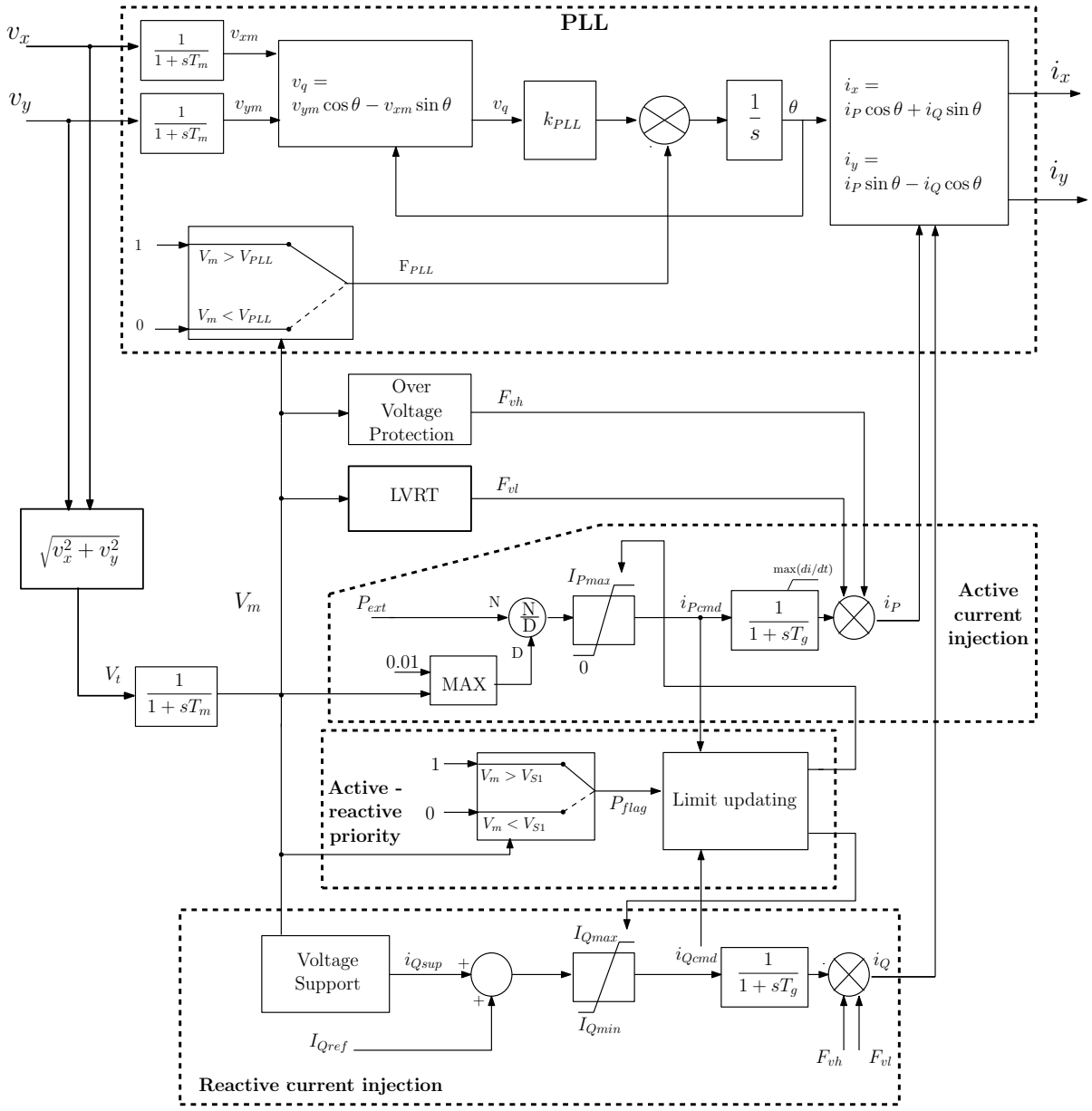

Figure 2. IBG generic model

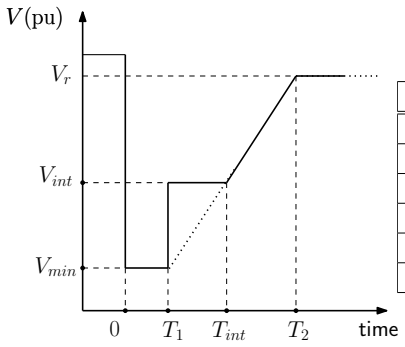

	Fig. 6.b	Fig. 6.a
V_r	0.9 pu	0.9 pu
V_{int}	0.7 pu	0.8 pu
V_{min}	0.2 pu	0.8 pu
T_1	0.2 s	1.5 s
T_{int}	0.7 s	$= T_1$
T_2	1.5 s	$= T_1$

Figure 3. Parameterized LVRT characteristic (fault occurring at $t = 0$)

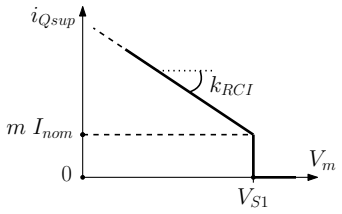

Figure 4. Parameterized characteristic of reactive current injection

B. Results with uniform distributions of parameters

MC simulations with uniform distribution of the random parameters (in the specified intervals) are first considered.

The procedure of Section II-C with $s_o = 100$ initial simulations, a tolerance $\delta = 0.01$ MVA and $g_{max} = 10$ led to generate $s = 757$ randomized responses to each of the eight disturbances.

Figures 8 and 9 show the 757 time evolutions of, respectively, the active and reactive powers received by the

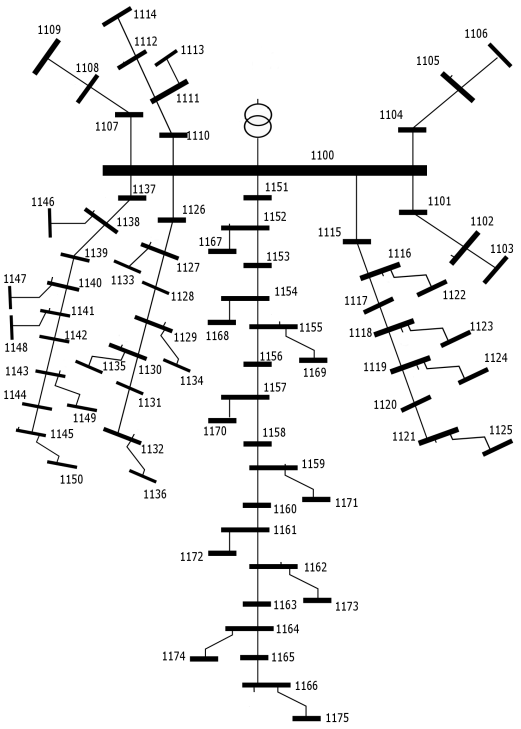

Figure 5. One-line diagram of the 75-bus 11-kV distribution network

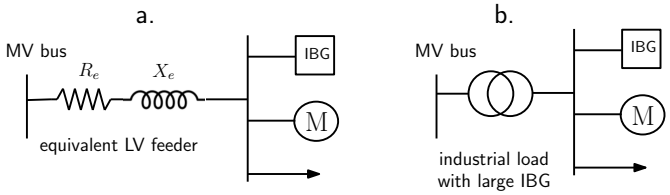

Figure 6. MV bus injection model: (a) equivalent LV feeder; (b) industrial load combined with a large PV unit

distribution grid at bus 1100 in response to disturbance No 1. Note that all responses correspond to the same operating point; hence, all curves start from the same value. The corresponding curves for disturbance No 8 are given in Figs. 10 and 11.

The reactive current injection during the fault by the IBGs at MV level can be seen in Figs. 9 and 11, with the power flow changing from import to export. But the most striking fact is the sharp increase of both the active and the reactive power immediately after fault clearing, even sharper for the voltage dip No. 8, which is deeper and lasts longer. The reason is twofold. First, the motors draw additional power when re-accelerating after fault clearing. Second, during the fault, the active currents of IBGs at MV level have been reduced, if not canceled, owing to the priority given to reactive currents for voltage support. The active power restoration of IBGs takes between one and two seconds and is clearly seen in the progressive reduction of the imported active power. Finally, it is noted that active power does not return to its pre-disturbance value. One reason is the tripping of the PV units connected to LV grids, allowed by their more permissive LVRT characteristic (see Fig. 3). Another reason is the randomization

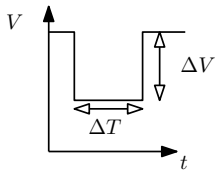

disturb. No	ΔV (pu)	ΔT (s)
1	0.5	0.10
2	0.5	0.25
3	0.6	0.10
4	0.6	0.25
5	0.7	0.10
6	0.7	0.25
7	0.8	0.10
8	0.8	0.25

Figure 7. Disturbances considered in the simulations

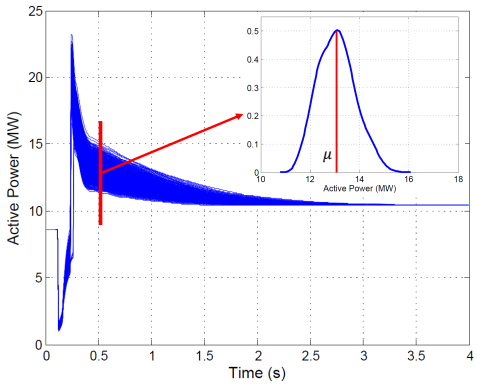

Figure 8. The 757 active power responses to disturbance No 1 (uniform distribution of parameters)

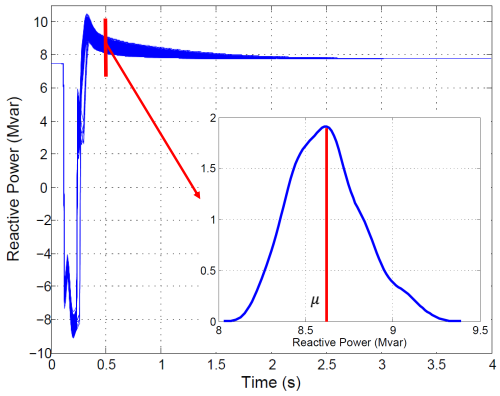

Figure 9. The 757 reactive power responses to disturbance No 1 (uniform distribution of parameters)

of the k_{RCI} parameter (see Fig. 4) resulting in smaller voltage support by some IBGs at MV level and, hence, a higher probability for the voltage to cross the LVRT characteristic.

Figures 8 to 11 also show the distributions of the 757 power values at $t = 0.5$ s (resp. $t = 1$ s) for voltage dip No 1 (resp. dip No 8). They are noticeably close to Gaussian distributions. The shown average μ corresponds to $\bar{P}$ or $\bar{Q}$ in Eqs. (1,2), for the disturbance and the discrete time considered.

The methods of Section II-B were applied to extract the $\boldsymbol{p}^\star$ parameter vector. Both methods proved to identify the same vector. The corresponding active (resp. reactive) power evolutions are shown in Fig. 12 (resp. 13), together with the averages $\bar{P}$ (resp. $\bar{Q}$) for the disturbance of concern. Apart

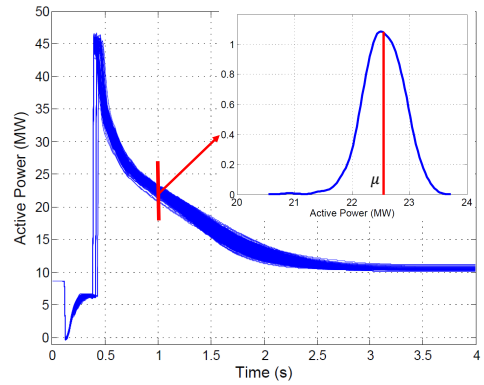

Figure 10. The 757 active power responses to disturbance No 8 (uniform distribution of parameters)

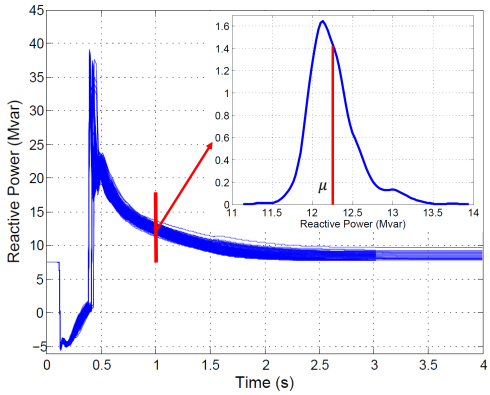

Figure 11. The 757 reactive power responses to disturbance No 8 (uniform distribution of parameters)

from short lasting spikes, the curves coincide very well.

C. Results with Gaussian distributions of parameters

The same procedure was repeated assuming Gaussian distributions for the parameters. As mentioned in Section II-A, the ranges of variation are the same for both distributions.

The procedure of Section II-C, with the same s_o, δ and g_{max} settings, led to generate $s = 577$ randomized responses, i.e. significantly less than for the uniform distributions.

Figures 14 and 15 show the 577 time evolutions of, respectively, the active and reactive powers received by the distribution grid in response to disturbance No 8 (shown alone, due to space limitations). The figures also show the distributions of the 577 power values at $t = 1$ s. In almost all cases, the responses are less dispersed around their averages, which makes sense in so far as the Gaussian distribution has a smaller standard deviation than the uniform one.

The power evolutions are similar. For the milder disturbances, the effect of active power recovery was found less pronounced.

Once again, the methods of Section II-B identified the same $\boldsymbol{p}^\star$ parameter vector. Figure 16 (resp. 17) compares the corresponding active (resp. reactive) power evolution with

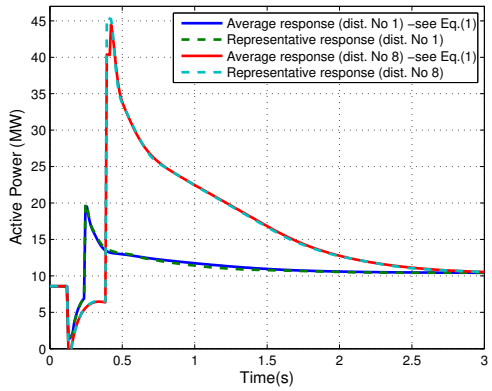

Figure 12. Active Power: average response $\bar{P}$ and evolution closest to this average (disturbances No 1 and 8, uniform distribution of parameters)

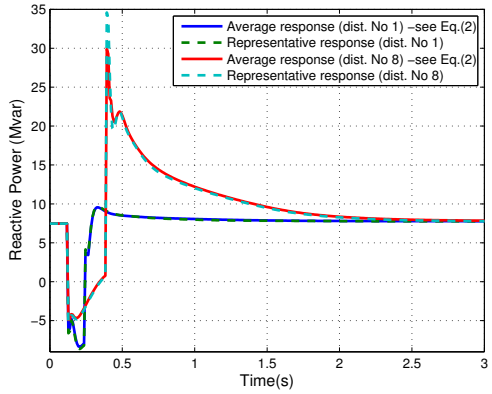

Figure 13. Reactive Power: average response $\bar{Q}$ and evolution closest to this average (disturbances No 1 and 8, uniform distribution of parameters)

the average evolution $\bar{P}$ (resp. $\bar{Q}$). Both coincide very well. Furthermore, comparing Fig. 16 with Fig. 12 (resp. Fig. 17 with Fig. 13) shows that the representative responses obtained respectively from the uniform and the Gaussian distributions are not identical but very close to each other.

V. Summary and Perspectives

This paper reports on efforts towards setting up a realistic ADN model, for use in simulations of large voltage disturbances in the transmission grid. It is assumed that the individual dynamic behaviour of IBGs and loads can be reasonably well captured by a generic model, but the values of its parameters are uncertain. The parameters are randomized in Monte-Carlo simulations, whose number is automatically determined. The outputs of interest are the active and reactive powers entering the ADN. Multiple disturbances are involved for better representativeness of the results. Two methods have been considered to identify the parameters which yield a dynamic response representative of the whole set. The latter was chosen to be the closest to the average evolution. In the tests, both methods were found equivalent.

Other criteria to select dynamic responses are worth being investigated. Let us quote, non exhaustively: choosing the response with the largest rate of change of power, using other

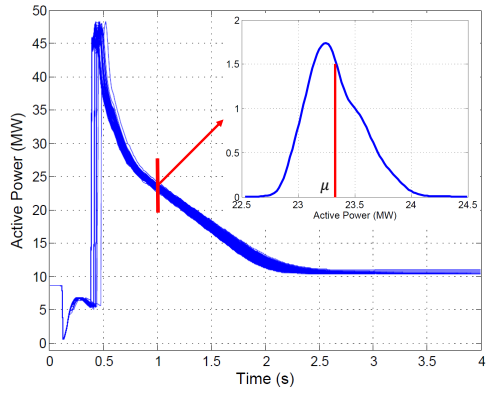

Figure 14. The 577 active power responses to disturbance No 8 (Gaussian distribution of parameters)

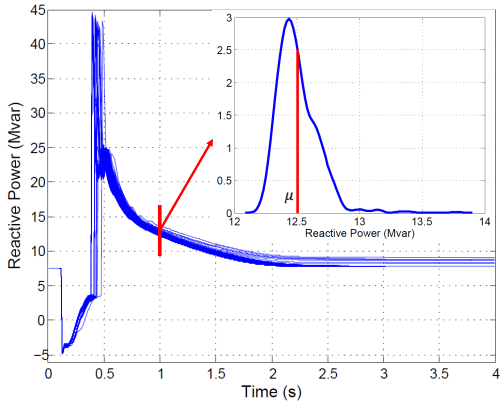

Figure 15. The 577 reactive power responses to disturbance No 8 (Gaussian distribution of parameters)

statistics than the average - such as the median - to build the reference evolution, or searching for the response which causes the largest stress to the transmission grid.

Another approach being investigated is the automatic clustering [12], [13] of the responses according to their similarities, with the objective of selecting one representative per cluster. One issue, however, is the unclear separation of the dynamic responses in the Monte-Carlo simulations generated so far.

The so obtained representative models will be subsequently used to derive dynamic equivalents of the ADN.

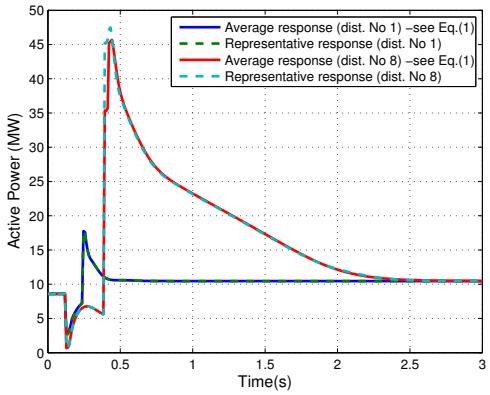

Figure 16. Active Power: average response $\bar{P}$ and the evolution closest to this average (disturbances No 1 and 8, Gaussian distribution of parameters)

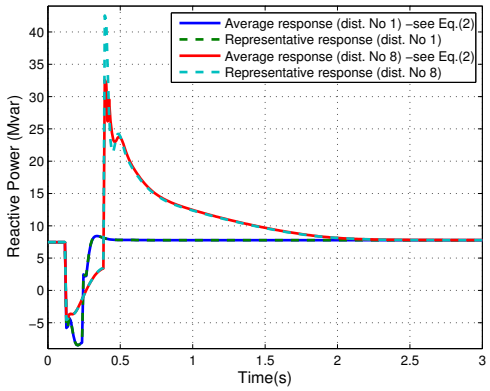

Figure 17. Reactive Power: average response $\bar{Q}$ and the evolution closest to this average (disturbances No 1 and 8, Gaussian distribution of parameters)

References

[1] C. Taylor, *Power System Voltage Stability*. Mc Graw Hill, EPRI Power Engineering Series, 1994.

[2] Y. Wang, W. Wu, B. Zhang, Z. Li, and W. Zheng, "Robust voltage control model for active distribution network considering pvs and loads uncertainties," 2015.

[3] K. Christakou, M. Paolone, and A. Abur, "Voltage control in active distribution networks under uncertainty in the system model: A robust optimization approach," *IEEE Transactions on Smart Grid*, vol. PP, no. 99, pp. 1–1, 2017.

[4] C. Z. Mooney, *Monte carlo simulation*, vol. 116. Sage Publications, 1997.

[5] I. A. Hiskens, M. Pai, and T. Nguyen, "Bounding uncertainty in power system dynamic simulations," *Proc. IEEE PES General Meeting*, vol. 2, pp. 1533–1537, 2000.

[6] S. M. Zali, N. Woolley, and J. Milanović, "Development of equivalent dynamic model of distribution network using clustering procedure," *Proc. 17th Power Systems Computation Conference*, 2011.

[7] G. Chaspierre, P. Panciatici, and T. Van Cutsem, "Dynamic Equivalent of a Distribution Grid Hosting Dispersed Photovoltaic Units," *Proc. IREP' 17 Symposium*, Espinho (Portugal), 2017, in press.

[8] VDE-AR-N 4120, "Technical requirements for the connection and operation of customer installations to the high-voltage network (TCC High-Voltage)," pp. 1–123, January 2015.

[9] B. Weise, "Impact of k-factor and active current reduction during fault-ride-through of generating units connected via voltage-sourced converters on power system stability," *IET Renewable Power Generation*, vol. 9, no. 1, pp. 25–36, 2015.

[10] H. Soleimani Bidgoli, M. Glavic, and T. Van Cutsem, "Receding-Horizon Control of Distributed Generation to Correct Voltage or Thermal Violations and Track Desired Schedules," *Proc. 19th PSCC conf.*, 2016.

[11] P. Aristidou, D. Fabozzi, and T. Van Cutsem, "Dynamic simulation of large-scale power systems using a parallel Schur-complement-based decomposition method," *IEEE Trans. on Parallel and Distributed Systems*, vol. 25, no. 10, pp. 2561–2570, 2014.

[12] D. Arthur and S. Vassilvitskii, "k-means++: The advantages of careful seeding," *Proc. 18th annual ACM-SIAM symposium on Discrete algorithms*, pp. 1027–1035, 2007.

[13] N. Pelekis, I. Kopanakis, E. E. Kotsifakos, E. Frentzos, and Y. Theodoridis, "Clustering uncertain trajectories," *Knowledge and Information Systems*, vol. 28, no. 1, pp. 117–147, 2011.